A comparative Study of Novel Extramedullary Fixation and Dynamic Hip Screw in the Fixation of Intertrochanteric Fracture: A Finite-Element Analysis

Kai Ding[1,2†], Yanbin Zhu[1,2†], Haicheng Wang[1,2], Yonglong Li[1,2], Weijie Yang[1,2], Xiaodong Cheng[1,2], Yingze Zhang[1,2,3,4], Wei Chen[1,2,3]* and Qi Zhang[1,2]*

[1]Trauma Emergency Center, The Third Hospital of Hebei Medical University, Shijiazhuang, China, [2]Key Laboratory of Biomechanics of Hebei Province, Orthopaedic Research Institute of Hebei Province, Shijiazhuang, China, [3]NHC Key Laboratory of Intelligent Orthopaedic Equipment, the third hospital of hebei medical university, Shijiazhuang, China, [4]Chinese Academy of Engineering, Bingjiaokou Hutong, Beijing, China

Background: Dynamic hip screw (DHS) is one of the most widely internal fixations for stabilizing intertrochanteric fracture, however, with a high risk of postoperative complications. The triangle support fixation plate (TSFP) is developed to reduce the postoperative complications. The purpose of study is to evaluate the biomechanical performance of the DHS and TSFP and demonstrate the rationality of triangular internal fixation for stabilizing intertrochanteric fractures.

Methods: The CT data of the proximal femur were used to establish finite-element models. Evans type I and IV intertrochanteric fracture were constructed and stabilized with the DHS and TSFP. The Von-Mises stress, maximum principal stress, minimum principal stress, and displacement were used to evaluate the biomechanical effect of two implants on intertrochanteric fracture.

Results: Under a 600N axial load, the maximum stress and displacement of an intact proximal femur were 13.78 MPa and 1.33 mm, respectively. The peak stresses of the bone in the TSFP were 35.41 MPa and 68.97 MPa for treating Evans type I and IV intertrochanteric fractures, respectively, which were lower than those in the DHS. The maximum overall displacement and relative distance of the fracture surface in the DHS fixation model were 1.66 mm and 0.10 mm for treating Evans type I intertrochanteric fracture, which was 29.59% and 150% higher than that in the TSFP, and were 2.24 mm and 0.75 mm for treating Evans type IV intertrochanteric fracture, which was 42.58% and 650% higher than that in the TSFP.

Conclusions: In conclusion, the TSFP has obvious advantages in stress distribution and stability than the DHS, providing a promising option for the treatment of intertrochanteric fractures.

Keywords: triangular structure, intertrochanteric fracture, finite-element analysis, biomechanical performance, DHS, TSFP

INTRODUCTION

As an osteoporosis-directly-related fracture, intertrochanteric fracture is highly prevalent in the elderly, accounting for approximately 3.4% of all fractures, and is expected to reach 4.6 million worldwide by the year 2050 (1, 2). Compared with the other type of hip fracture, femoral neck fracture, intertrochanteric fractures are associated with a higher risk of postoperative complications including mortality, with the latter reported at rates ranging from 11% to 29% within one year (3–6). Early surgical treatment within 24–48 h after injury is recommended as the standard intervention method to achieve quick functional recovery and reduced postoperative complications (7).

Among various operative methods, open reduction with DHS fixation is considered the gold standard for the treatment of stable intertrochanteric fractures (8–10). From the point of view of biomechanics, the DHS and other techniques reconstruct the anatomical structure of the tension trabeculae, and the fulcrum shifts outward, increasing the length of the force arm. The above internal fixation does not reconstruct the fracture of the tension line of the proximal femur (11, 12). Even if a slight load is applied to the femoral head, it can be amplified at the nail and plate, which can easily cause backout and hip inversion. Due to the limitations of the DHS per se in design, the DHS is related to various postoperative complications, including withdrawal, cut-out, and varus collapse, with fixation-failure rates of 1.5%–21%. It is suggested that posteromedial cortical integrity is critical to the clinical prognosis for the DHS fixing intertrochanteric fractures (13–16). In addition, lateral cortical integrity contributes greatly to stability, and the loss of lateral cortical integrity is reported to be associated with up to a 6-time risk of reoperation (10, 17).

Analyses of these failure cases indicated that the single fixation screw of the DHS could not support adequate force to counteract the fractured trabeculae, leading to direct hardware-related complications, and the ideal internal fixation devices should first be able to address this problem.

In this study, we will present our innovation, the TSFP, where the supporting screw is added to form a stable triangular structure with the main plate and fixing screw, thus enhancing the ability to resist the tension and compression force at the proximal femur (18–21). In 2009, our research team first proposed the concept of triangular support fixation that the anti-tension screw was added to form a double triangular structure with the main plate and anticompression screw (18, 19), and 3 Chinese granted patents were obtained (ZL200920254063.4, ZL200920254062.x, ZL201120370391.8). Theatrically, this will reduce the dependence on posteromedial and lateral cortical integrity and further minimize the occurrence of hardware-related complications.

In this study, our main aim was to compare the stress distribution and stability of two implant fixation models by using finite-element analysis and verify whether the innovated triangular support fixation could have superior biomechanics of intertrochanteric fractures compared with the traditional DHS. Finite-Element Analysis (FEA) is a numerical analysis method to simulate the real physical system (geometry and load conditions) by using mathematical approximation. It is widely used in the trauma field because of its advantages of simple operation, convenient model acquisition, and strong experimental reliability (11, 12, 22).

METHODS AND MATERIAL

The study protocol was approved by the Institutional Review Board (IRB) and conformed to the provisions of the Declaration of Helsinki. Written informed consent was obtained from the volunteers prior to the study commencement.

Three-Dimensional Models

A healthy volunteer (male, age 27 years, height 173 cm, and body weight 60 kg) without a history of lower extremity injury was included. The volunteer underwent a 64 slice spiral CT scan (SOMATOM Definition AS Siemens, Germany) with a slice of 0.625 mm from the hip joint to the knee joint. The CT data were used to establish a three-dimensional model of the proximal femur in Mimics 21.0 (Materialise company, Leuven,). The proximal femoral model was imported into Geomagic 13.0 (Geomagic company, USA) to generate the solid models. Hypermesh 2014 (Altair Company, USA) was used to mesh the solid model with C3D4 elements.

According to their real dimensions, the DHS and TSFP were constructed by UG-NX 12.0 (Siemens Company, USA). The length, dimension, and angle of the DHS and TSFP are demonstrated in **Figure 1** (**Figures 1**, **2**). We considered Evans I and IV intertrochanteric fractures as typically stable and unstable intertrochanteric fractures, respectively. To brief the research plan of this study, Evans type I and IV intertrochanteric fractures were included. These fractures were created and stabilized with the DHS and TSFP in UG-NX 12.0, respectively. The key point of the TSFP was an added supporting screw, which constituted a cross-structure with the locking screw through the fitting hole (sliding hole or threaded hole), forming a double triangle fixation of the main plate, locking screw, and supporting screw in a three-dimensional space.

Material Properties

The models were imported into Abaqus6.14(Dassault Systèmes Solid Works Corp., Concord, MA, USA). The bone and implant were set as homogeneous, isotropic, and linear elastic materials. On the basis of previous literature, the Young's modulus of the cortical and cancellous bone was 17 GPa and 1.5 GPa, while the Poisson's ratio was 0.3 for both (23, 24). The Young's modulus and Poisson's ratio of the implant were 110 GPa and 0.316 (25), respectively.

Boundary Conditions

The full bonding was used as an interface between the supporting screw, fixating screw, and main plate in the TSFP model. The interfaces between the screw and the plate were assumed as fully bonding in the DHS model. The tied
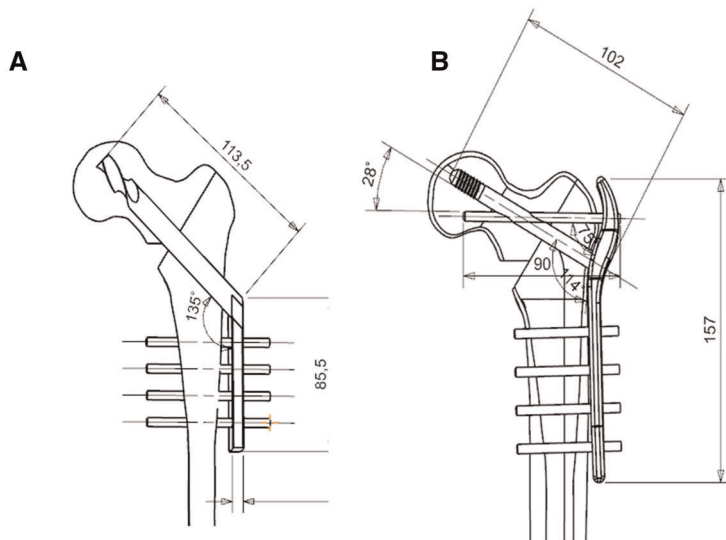
FIGURE 1 | Diagram, detail, and specifications of internal fixation devices; (**A**) DHS; and (**B**) TSFP.

interactions between screw thread/bone and screw/ cortical bone were used to mimic the holding force. Other bone–screw and bone–bone interfaces were assumed as surface-to-surface contact relation. The friction coefficient was set as 0.3 (18, 26, 27). In this experiment, loads were applied using distributed coupling constraints. A concentrated force load was applied at the reference point, i.e., vertically above the femoral head. All construct models were applied with a load of 600N (one leg standing load force). The distal end of the femoral model was completely fixed in all degrees of freedom (**Figure 3**).
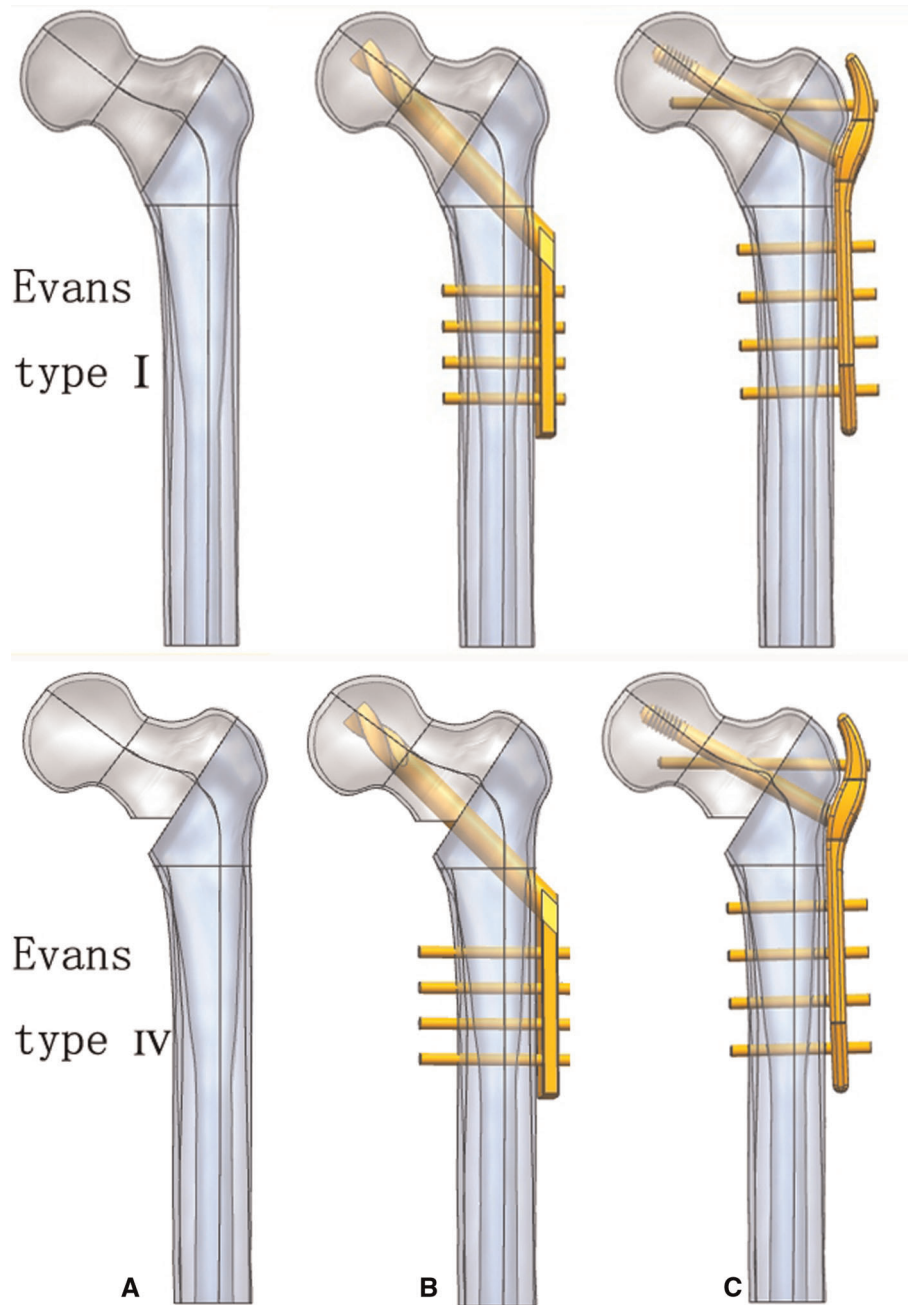
FIGURE 2 | Geometric modeling of stable and unstable intertrochanteric fracture models and three implant fixation models; (A) the Evans type I and IV intertrochanteric fractures; (B) DHS fixation model; and (C) TSFP fixation model.

Validation of Finite-Element Models

In this study, we tested the maximum von-Mises stress on the cancellous and cortical bones of the proximal femur to analyze mesh convergence and validate the model. The selected method was widely used in the convergence test (27, 28). The convergence criterion used was a change of <5%.

The final model was made of 7,564 nodes and 93,332 elements (mesh size: 2 mm) (Figure 4).

The finite-element model was validated with a biomechanical study where the proximal femoral bone was fixed under the same boundary conditions. Femur specimens were selected from donated male cadavers. Specimens with rheumatism,

FIGURE 3 | Boundary conditions of the models.

tuberculosis, tumors, or abnormal bone quality were excluded using imaging examinations. The biomechanical testing machine (BOSE ElectroForce 3520-AT, BOSE Company, USA) was used to apply load. A 16-channel stress–strain tester (m + p, Hannover, Germany) and strain gauges (BF3503AA, Chengdu,

China) were used to detect and record the stains of marker points. The strain values of nine marked points in the specimen were collected to compare with those in the finite-element analysis. From the comparison of the results, we found that our finite-element model of proximal femur was reliable and effective (**Figures 5**, **6** and **Table 1**).

RESULTS

The Von Mises Stress and Displacement Distribution of the Intact Bone

The maximum stress of the intact bone was 13.78 MPa, which was located at the medial femoral cortex. The maximum stress of the lateral femoral cortex was 6.31 MPa. The maximum displacement was 1.33 mm (**Figure 7**).

The Von Mises Stress, Maximum Principal Stress, and Minimum Principal Stress Distribution of the DHS and TSFP Models for the Fixation of Evans Type I and IV Intertrochanteric Fracture

For the DHS and TSFP groups, a stress concentration of the medial and lateral femoral cortex occurred around the fracture and the hole adjacent to the main plate, respectively. The Von Mises stress, maximum principal stress, and minimum principal stress concentration of the DHS were located at the junction of the fixation screw and plate and those of the TSFP were placed on the junction of the supporting screw, fixating screw, and main plate.

For Evans type I intertrochanteric fracture, the maximum mises stresses of the medial cortex, lateral cortex, and implant in the DHS were 1.19 times, 2.55 times, and 1.15 times greater than those in the TSFP, respectively. The DHS was 1.08 times and 1.11 times as much minimum and maximum principal stress extreme as the TSFP (**Figures 8–11** and **Tables 2–4**).

For Evans type IV intertrochanteric fracture, the maximum mises stresses of the medial cortex, lateral cortex, and implant in the DHS were 41.66%, 4.99 times, and 1.70 times as much as that in the TSFP, respectively. The DHS was 1.51 times and 1.65 times as much minimum and maximum principal stress extreme as the TSFP (**Figures 8–11** and **Tables 2–4**).

The Displacement Distribution of Two Implants for Treatment of Evans Type I and IV Intertrochanteric Fracture

For two variations, the maximum displacement values of the DHS for stabilizing Evans type I and IV intertrochanteric fractures were 1.66 mm and 2.24 mm and those of the TSFP were 1.28 mm and 1.57 mm, respectively.

The maximum relative displacements of the fracture surface of the DHS for fixing Evans type I and IV intertrochanteric fractures were 0.10 mm and 0.75 mm, respectively, and those of the TSFP were 0.04 mm and 0.10 mm, respectively (**Figures 8**, **9** and **Tables 2**, **3**).
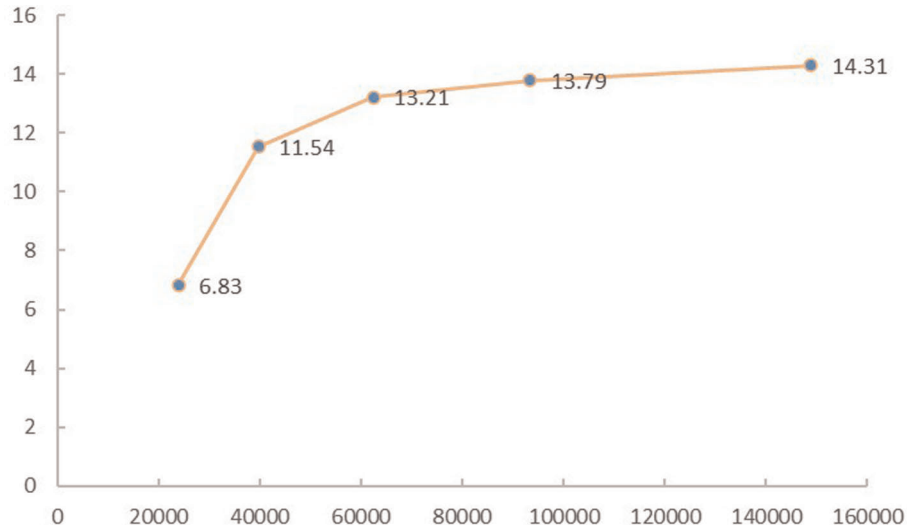
FIGURE 4 | The von Mises stress on the cancellous and cortical bone of the proximal femur was tested to analyze the mesh convergence and validate the model.
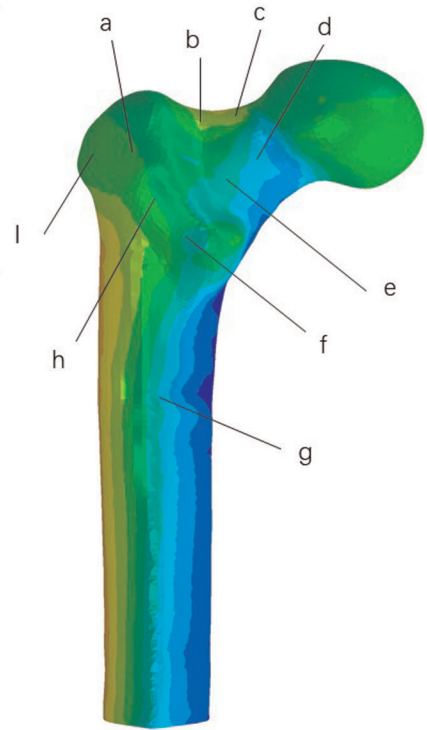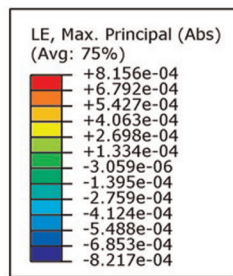

FIGURE 5 | Results of the validated experiment. (**A**): biomechanical study; and (**B**): finite-analysis element.

DISCUSSION

In the current study, we found that the TSFP showed superior biomechanical performances, including reducing the reliance of the DHS on the posteromedial and lateral femoral cortex, increasing the construct stability, and improving the stress distribution of the implant. The main reason for the improved biomechanics of the implant construct model is the cross structure of the supporting and fixating screws. The concept of triangular support fixation would be important to improve
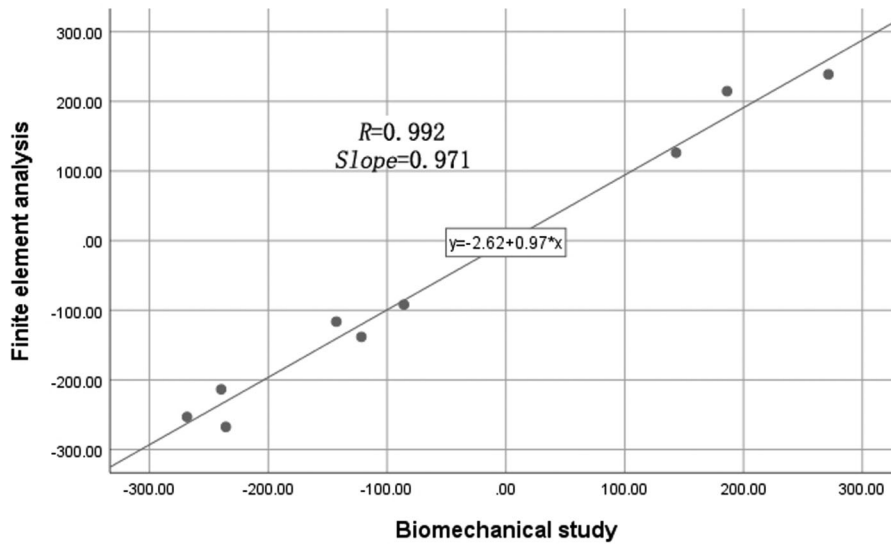
FIGURE 6 | Recording the strain value of marker points in the biomechanical study and finite-element analysis.

TABLE 1 | The strain values of the biomechanical test and finite-element analysis (10^{-6}).

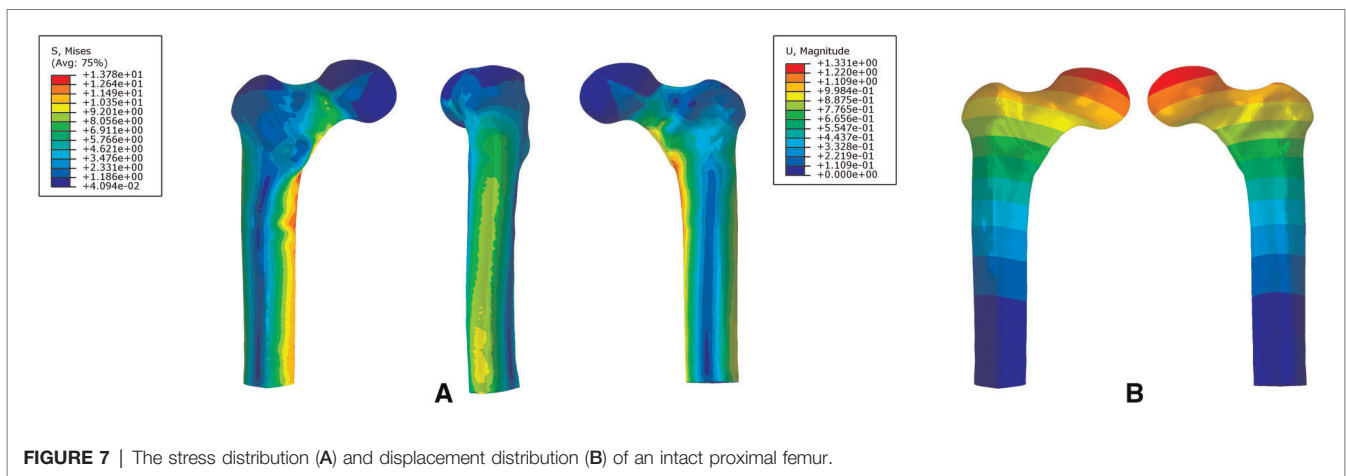| Maker point	a	b	c	d	e	f	g	h	i
Finite-element analysis	126.32	238.87	214.65	−253.24	−116.37	−267.54	−213.54	−91.94	−138.25
Biomechanical study	143.26	271.46	186.15	−268.39	−142.74	−235.74	−239.62	−85.83	−121.62

FIGURE 7 | The stress distribution (**A**) and displacement distribution (**B**) of an intact proximal femur.

clinical outcomes and reduce postoperative complications in treating various intertrochanteric fractures.

The TSFP provides a better biomechanical performance than the DHS in terms of mechanical aspects. This is due to the unique double triangular structure of the TSFP. First, the first triangle is composed of the cancellous bone of the femoral head, supporting screw, and fixing screw, which is called a mixed triangle. The second triangle, called a metal triangle, is constructed by simulating the triangular cantilever structure of the proximal femur which is made up of the supporting screw, fixing screw,

and main plate. The fixing and supporting screws are kept in line with the spatial position and orientation of the trabecular system of the proximal femur. According to our result, the TSFP has less relative distance of fracture section, which shows that the mixed triangular structure can obviously improve the holding force of the fracture fragment. Secondly, the metal triangle plays the similar role of the screw-plate joint of the DHS, and three fulcrums of the metal triangle greatly disperse the stress concentration of the screw-plate joint. Moreover, the supporting screw and main plate together support the fixing
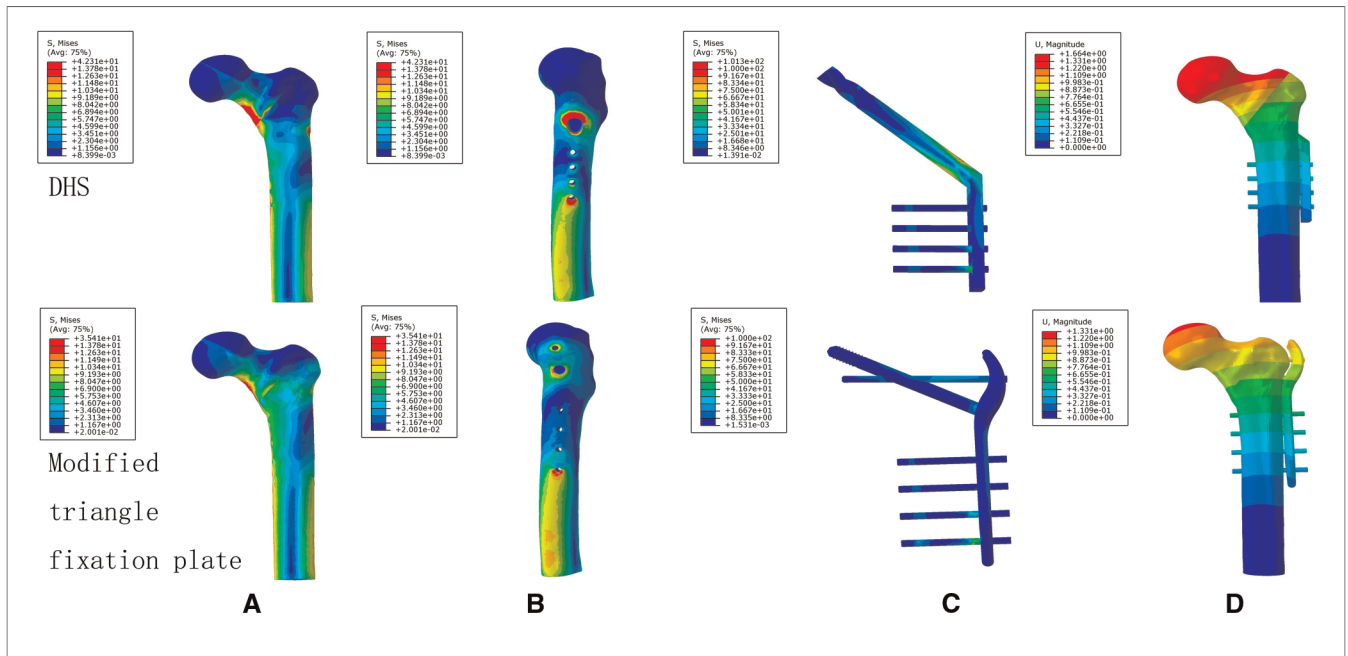
FIGURE 8 | The stress distribution and displacement distribution of two implant fixations of a stable intertrochanteric fracture; **(A)** the stress distribution of bone models; **(B)** the stress distribution of the lateral femoral cortex; **(C)** the stress distribution of an implant model; **(D)** the displacement distribution of three implant fixation models. The figure shows that the TSFP has improved the stress distribution of the implant and bone models and increased the construct stability of the fixation of Evans type I intertrochanteric fracture.

FIGURE 9 | The stress distribution and displacement distribution of two implant fixations of an unstable intertrochanteric fracture; **(A)** the stress distribution of bone models; **(B)** the stress distribution of the lateral femoral cortex; **(C)** the stress distribution of an implant model; **(D)** the displacement distribution of three implant fixation models. The figure shows that the TSFP has improved the stress distribution of the implant and bone models and increased the construct stability of the fixation of Evans type IV intertrochanteric fracture.
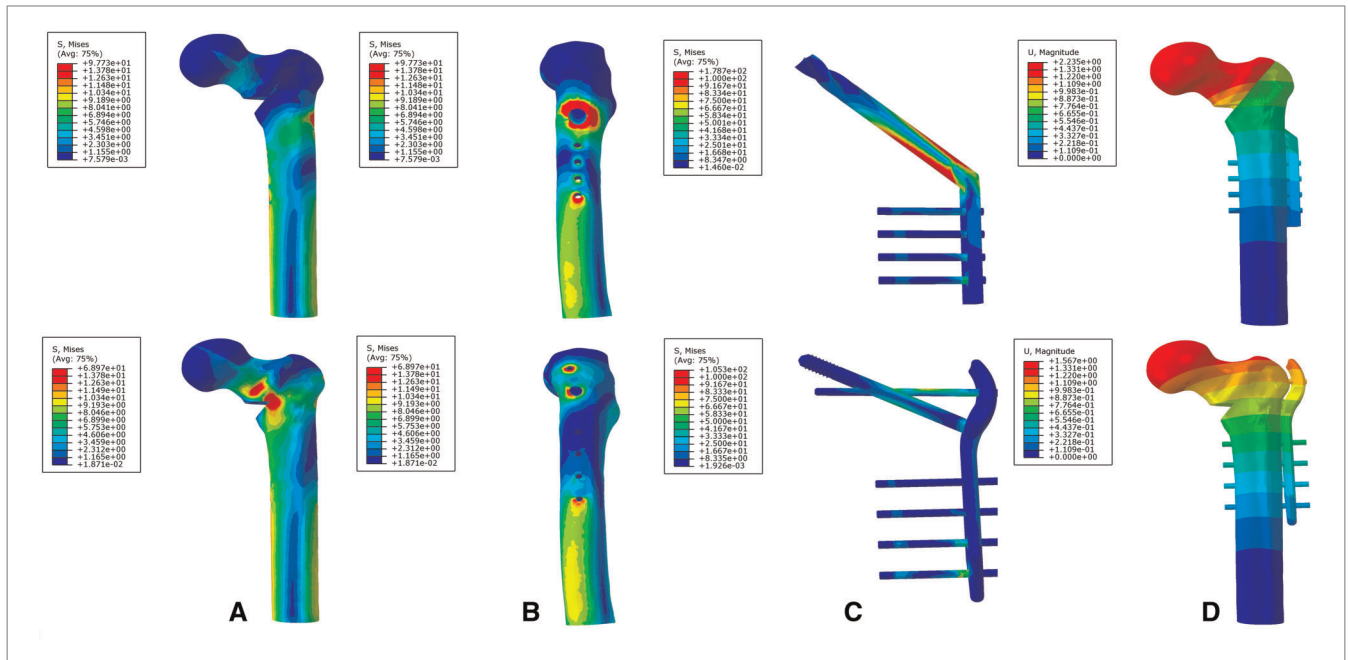
screw, forming a double-pivot fixation to improve the overall stability of the intertrochanteric fracture. The triangle structure of the TSFP has better resistance to the tension and compression force in the proximal femur than the single fixing

screw, reducing tension and compression force component to the femur which has lower requirement on the integrity of femoral posteromedial and lateral cortex. The double triangular structure perfectly solves the stress concentration of the

FIGURE 10 | The maximum principal stress and minimum principal stress extremes of two implant models for the treatment of a stable intertrochanteric fracture. The figure shows that the TSFP has improved the maximum principal stress distribution compared with DHS for the fixation of Evans type I intertrochanteric fracture.
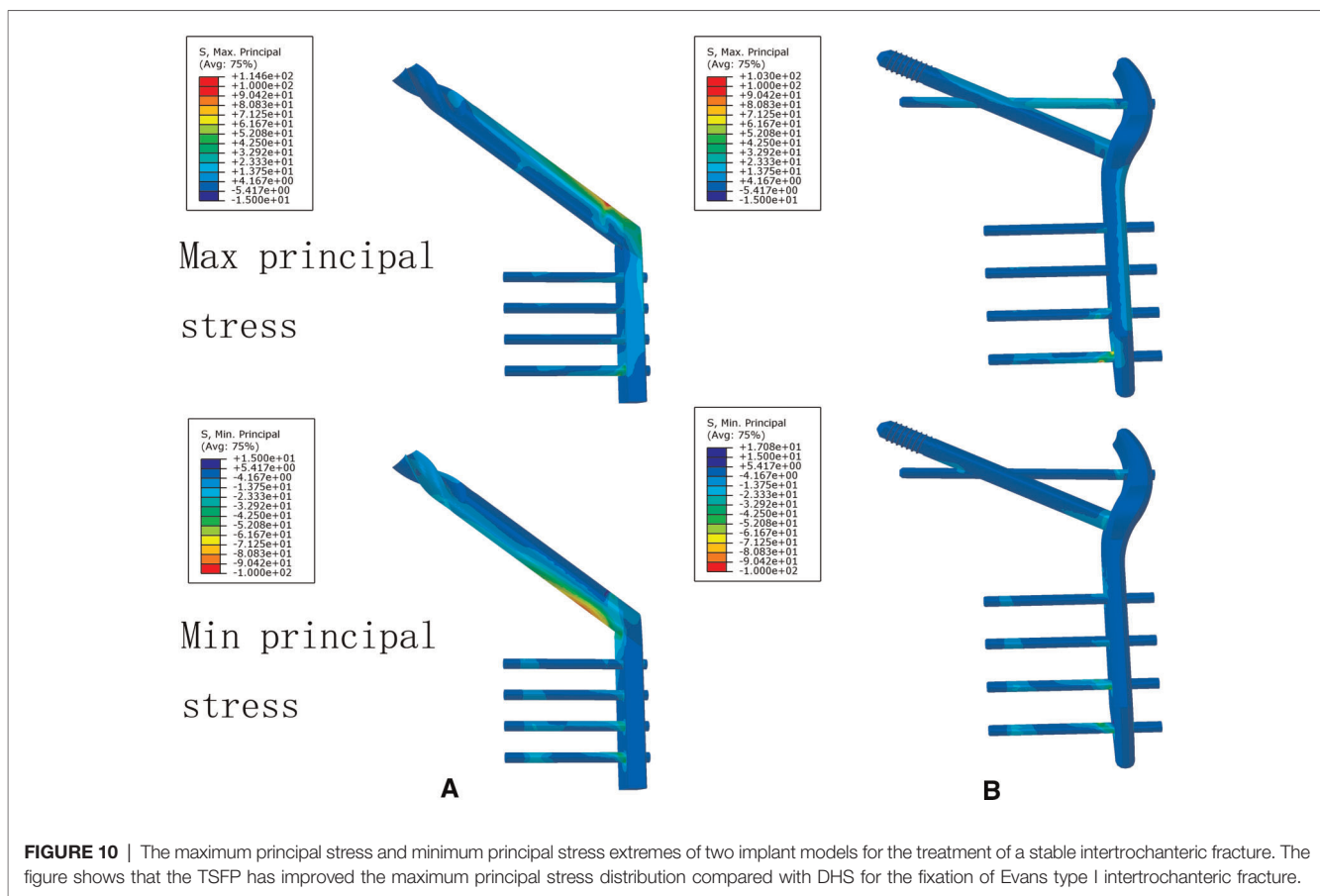
screw-plate junction, reduces excessive dependence on the posteromedial and lateral cortex, and increases the stability of the fracture fixation model compared with the DHS, which has important clinical implications for reducing the risk of postoperative reduction loss, varus collapse, screw cut-out, and so on.

The biomechanical difference between the DHS and the TSFP was a result of varying the fixation mechanism for intertrochanteric fracture. The fixation mechanism of the DHS for intertrochanteric fracture was summarized as "two points and one line." That is, one line is the fixing screw, and the two points are the posteromedial and lateral cortex of the proximal femur. Due to a huge bending moment of the proximal femur, body loading was transmitted to the tension and compression force, which single fixation screw could not fully counteract. Also, the posteromedial and lateral cortex in the proximal femur act as fulcrums to counteract the tension and compression force component, respectively. Biomechanically, only if the support of both posteromedial and lateral femoral cortex is maintained, the DHS fixation of intertrochanteric fractures will be safe (29). Therefore, the peak stresses of the posteromedial and lateral femoral cortex in the DHS fixation model were 42% and 4.99 times of those in the TSFP for treating an unstable intertrochanteric fracture, which could be explained by the fact that the DHS construct model had a higher instability and separation of the fracture fragment than that of the TSFP with

the loss of the posteromedial femoral cortex. The triangle structure is more suitable for intertrochanteric fracture than for a single fixing screw.

The literature review showed that clinical effects were increasing with the continuous development of extramedullary devices from the DHS to the MSP (Medoff sliding plate) and the LCP to the PCCP (percutaneous compression plating system) (30). However, the above instrument was not currently used for the main treatment of intertrochanteric fracture. Although the MSP and LCP increased the construct stability and reduced the risk of fixation-related complications, intraoperative soft tissue dissection and bleeding were difficult to avoid because of the complex surgical procedure (31–33). The PCCP achieved a minimally invasive procedure, but its double parallel lag screw still could not solve the long lever arm and stress concentration of the screw-plate junction (34, 35). Intramedullary fixation has gradually become the mainstream treatment for intertrochanteric fractures due to minimal invasion, small soft tissue injury, and shortening of the long arm (36, 37). However, the single fixing screw of Gamma nail and PFNA was also not counteracted with the tension and compression force of the proximal femur like the DHS, leading to an overreliance on the femoral cortex, whose fixation-related failures reached between 2.5% and 12.5% (30, 38–40). Although there was an in-depth understanding of the trabecular system of proximal femur, the concept of triangular
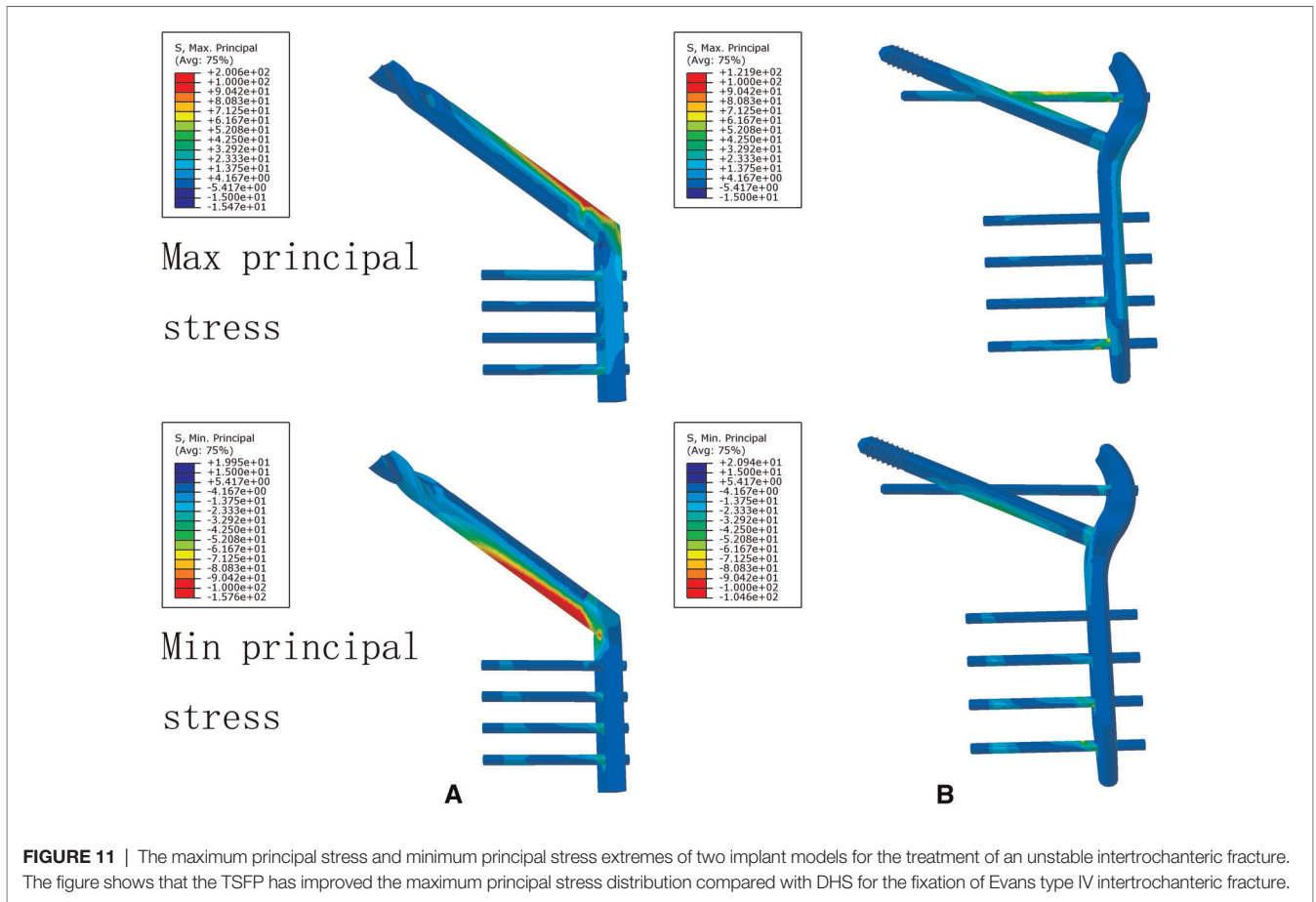
FIGURE 11 | The maximum principal stress and minimum principal stress extremes of two implant models for the treatment of an unstable intertrochanteric fracture. The figure shows that the TSFP has improved the maximum principal stress distribution compared with DHS for the fixation of Evans type IV intertrochanteric fracture.

TABLE 2 | The maximum displacement and stress values of two implant models for the treatment of stable intertrochanteric fracture.

Implant models	Maximum stress (MPa)			Maximum displacement (mm)	
	Medial cortex	**Lateral cortex**	**Implant**	**Fixation models**	**Relative fracture surface**
DHS	42.31	39.14	101.28	1.66	0.10
TSFP	35.41	15.36	88.02	1.28	0.04

TABLE 3 | The maximum displacement and stress values of two implant models for the treatment of an unstable intertrochanteric fracture.

Implant models	Maximum stress (MPa)			Maximum displacement (mm)	
	Medial cortex	**Lateral cortex**	**Implant**	**Fixation models**	**Relative fracture surface**
DHS	28.73	97.73	178.74	2.24	0.75
TSFP	68.97	19.58	105.31	1.57	0.10

support fixation was first put forward by our research team, and 3 Chinese granted patents were obtained in 2009. The TSFP had high stability, combining the advantages of intramedullary and

TABLE 4 | The maximum principal stress and minimum principal stress distribution of two implant models for the treatment of unstable and stable intertrochanteric fractures (MPa).

Implant models	Stable intertrochanteric fracture		Unstable intertrochanteric fracture	
	Max principal stress	**Min principal stress**	**Max principal stress**	**Min principal stress**
DHS	114.61	−89.65	200.63	−157.63
TSFP	103.04	−83.28	121.92	−104.55

extramedullary fixation. We considered that the TSFP was a bionic internal fixation of the proximal femur, which could be suitable for various intertrochanteric fractures, and had a great impact on the prognosis of intertrochanteric fractures. Finally, we will also carry out the biomechanical and clinical studies of the TSFP and promote the clinical application of the TSFP in intertrochanteric fracture.

There are some limitations in this study. First, the properties of the bone were set as homogeneous, isotropic, and linear elastic behavior, which were different from those of the actual bone. However, the bone model was validated with the biomechanical study, and the difference was within the acceptable range ($R = 0.992$, *Slope* $= 0.971$). Second, we

explored the optimal biomechanical effects of the different implantation points of the supporting screw versus the fixation screw in the lateral wall on intertrochanteric fractures. Third, because different intertrochanteric fractures have its own unique characteristics, the absence of an Evans II/III/V intertrochanteric fractures model in this study limited the value of our research. Finally, the four-hole side-plate DHS selected in the study was one fixation type in clinical practice, but to the question whether the DHS was the optimal fixation for intertrochanteric fractures, there was a lack of biomechanical and clinical evidence (41–43). In addition, the DHS has a variety of structures and material properties, which may impact the results of this study.

In conclusion, the TSFP reduced dependence on the femoral posteromedial and lateral cortex and improved the stability and stress distribution of the construct model. The TSFP conformed to the biomechanical characteristics of the proximal femur, which is a promising internal fixation for intertrochanteric fractures.

DATA AVAILABILITY STATEMENT

The original contributions presented in the study are included in the article/Supplementary Material; further inquiries can be directed to the corresponding author/s.

ETHICS STATEMENT

This study has been reviewed and approved by the Institutional Review Board of The Third Hospital of Hebei Medical University. Written informed consent was provided by the participants.

All authors have read and contributed to the submitted manuscript and have no conflict of interest to declare. Identifying images or other personal or clinical details of participants are not presented.

AUTHOR CONTRIBUTIONS

KD, LY, XC, and HW analyzed and interpreted the data. KD, WC, and YZ wrote the manuscript. WC, YZ, and QZ contributed most to the revision of this manuscript. QZ WC, and YZ designed the study. QZ and WC conducted the search for relevant studies. All authors contributed to the article and approved the submitted version.

FUNDING

REFERENCES

1. Chen W, Lv H, Liu S, Liu B, Zhu Y, Chen X, et al. National incidence of traumatic fractures in China: a retrospective survey of 512 187 individuals. *Lancet Glob Health*. (2017) 5:e807–17. doi: 10.1016/s2214-109x (17)30222-x

2. Gullberg B, Johnell O, Kanis JA. World-wide projections for hip fracture. *Osteoporos Int*. (1997) 7:407–13. doi: 10.1007/pl00004148

3. Keyak JH, Falkinstein Y. Comparison of in situ and in vitro CT scan-based finite element model predictions of proximal femoral fracture load. *Med Eng Phys*. (2003) 25:781–7. doi: 10.1016/s1350-4533(03)00081-x

4. Guzon-Illescas O, Perez Fernandez E, Crespí Villarias N, Quirós Donate FJ, Peña M, Alonso-Blas C, et al. Mortality after osteoporotic hip fracture: incidence, trends, and associated factors. *J Orthop Surg Res*. (2019) 14:203. doi: 10.1186/s13018-019-1226-6

5. Kannegaard PN, van der Mark S, Eiken P, Abrahamsen B. Excess mortality in men compared with women following a hip fracture. National analysis of comedications, comorbidity and survival. *Age Ageing*. (2010) 39:203–9. doi: 10.1093/ageing/afp221

6. Elis J, Chechik O, Maman E, Steinberg EL. Expandable proximal femoral nails versus 95° dynamic condylar screw-plates for the treatment of reverse oblique intertrochanteric fractures. *Injury*. (2012) 43:1313–7. doi: 10.1016/j. injury.2012.05.004

7. Kokoroghiannis C, Aktselis I, Deligeorgis A, Fragkomichalos E, Papadimas D, Pappadas I. Evolving concepts of stability and intramedullary fixation of intertrochanteric fractures–a review. *Injury*. (2012) 43:686–93. doi: 10.1016/ j.injury.2011.05.031

8. Babhulkar S. Unstable trochanteric fractures: Issues and avoiding pitfalls. *Injury*. (2017) 48:803–18. doi: 10.1016/j.injury.2017.02.022

9. Parker MJ, Handoll HH. Gamma and other cephalocondylic intramedullary nails versus extramedullary implants for extracapsular hip fractures in adults.

Cochrane Database Syst Rev. (2005) 19:Cd000093. doi: 10.1002/14651858. CD000093.pub3

10. Palm H, Jacobsen S, Sonne-Holm S, Gebuhr P. Integrity of the lateral femoral wall in intertrochanteric hip fractures: an important predictor of a reoperation. *J Bone Joint Surg Am*. (2007) 89:470–5. doi: 10.2106/jbjs.F.00679

11. Mahaisavariya B, Chantarapanich N, Riansuwan K, Sitthiseripratip K. Prevention of excessive medialisation of trochanteric fracture by a buttress screw: a novel method and finite element analysis. *J Med Assoc Thai*. (2014) 97(Suppl 9):S127–32.

12. Jitprapaikulsarn S, Chantarapanich N, Gromprasit A, Mahaisavariya C, Patamamongkonchai C. Single lag screw and reverse distal femur locking compression plate for concurrent cervicotrochanteric and shaft fractures of the femur: biomechanical study validated with a clinical series. *Eur J Orthop Surg Traumatol*. (2021) 31:1179–92. doi: 10.1007/s00590-020-02868-z

13. Jensen JS, Sonne-Holm S, Tøndevold E. Unstable trochanteric fractures. A comparative analysis of four methods of internal fixation. *Acta Orthop Scand*. (1980) 51:949–62. doi: 10.3109/17453678008990900

14. Clawson DK. Trochanteric fractures treated by the sliding screw plate fixation method. *J Trauma*. (1964) 4:737–52. doi: 10.1097/00005373-196411000-00001

15. Mulholland RC, Gunn DR. Sliding screw plate fixation of intertrochanteric femoral fractures. *J Trauma*. (1972) 12:581–91. doi: 10.1097/00005373-197207000-00006

16. Wolfgang GL, Bryant MH, O'Neill JP. Treatment of intertrochanteric fracture of the femur using sliding screw plate fixation. *Clin Orthop Relat Res*. (1982):148–58.

17. Hsu CE, Shih CM, Wang CC, Huang KC. Lateral femoral wall thickness. A reliable predictor of post-operative lateral wall fracture in intertrochanteric fractures. *Bone Joint J*. (2013) 95-b:1134–8. doi: 10.1302/0301-620x.95b8. 31495

18. Ding K, Zhu Y, Li Y, Wang H, Cheng X, Yang W, et al. Triangular support intramedullary nail: A new internal fixation innovation for treating intertrochanteric fracture and its finite element analysis. *Injury*. (2022) 20: S0020-1383(22)00222-4. doi: 10.1016/j.injury.2022.03.032

19. Wang H, Yang W, Ding K, Zhu Y, Zhang Y, Ren C, et al. Biomechanical study on the stability and strain conduction of intertrochanteric fracture fixed with proximal femoral nail antirotation versus triangular supporting intramedullary nail. *Int Orthop*. (2022) 46:341–50. doi: 10.1007/s00264-021-05250-8

20. Zhu Y, Ding K, Li Y, Wang H, Chen W, Hou ZZ, et al. Biomechanical comparison of triangle supporting fixation system and Gamma nail fixation in the treatment of intertrochanteric fractures of the femur: finite element analysis. *Chin J Orthop*. (2021) 41:1361–6. doi: 10.3760/cma.j.cn121113-20210601-00394

21. Zhang YZ, Wang HC, Chen W, Zhu Y, Ding K, Hou ZZ, et al. Triangular supporting fixation: an innovative surgical approach for intertrochanteric fractures of the Temur – evidence from a biomechanical study. *Chin J Orthop Trauma!*. (2021) 23:461–6. doi: 10.3760/cma.j.cn115530-20210602-00255

22. Chantarapanich N, Riansuwan K. Biomechanical performance of short and long cephalomedullary nail constructs for stabilizing different levels of subtrochanteric fracture. *Injury*. (2022) 53:323–33. doi: 10.1016/j.injury.2021.11.064

23. Ding K, Yang W, Wang H, Zhan S, Hu P, Bai J, et al. Finite element analysis of biomechanical effects of residual varus/valgus malunion after femoral fracture on knee joint. *Int Orthop*. (2021) 45:1827–35. doi: 10.1007/s00264-021-05039-9

24. Cun Y, Dou C, Tian S, Li M, Zhu Y, Cheng X, et al. Traditional and bionic dynamic hip screw fixation for the treatment of intertrochanteric fracture: a finite element analysis. *Int Orthop*. (2020) 44:551–9. doi: 10.1007/s00264-019-04478-9

25. Ding K, Yang W, Zhu J, Cheng X, Wang H, Hao D, et al. Titanium alloy cannulated screws and biodegradable magnesium alloy bionic cannulated screws for treatment of femoral neck fractures: a finite element analysis. *J Orthop Surg Res*. (2021) 16:511. doi: 10.1186/s13018-021-02665-2

26. Tsuang FY, Hsieh YY, Kuo YJ, Chen CH, Lin FH, Chen CS, et al. Assessment of the suitability of biodegradable rods for use in posterior lumbar fusion: an in-vitro biomechanical evaluation and finite element analysis. *PLoS One*. (2017) 12:e0188034. doi: 10.1371/journal.pone.0188034

27. Li M, Zhao K, Ding K, Cui YW, Cheng XD, Yang WJ, et al. Titanium alloy gamma nail versus biodegradable magnesium alloy bionic gamma nail for treating intertrochanteric fractures: a finite element analysis. *Orthop Surg*. (2021) 13:1513–20. doi: 10.1111/os.12973

28. Zhan S, Jiang D, Xu J, Ling M, Yang K, Li Y, et al. Influence of the proximal screws of buttress plates on the stability of vertical femoral neck fractures: a finite element analysis. *BMC Musculoskelet Disord*. (2020) 21:842. doi: 10.1186/s12891-020-03853-7

29. Socci AR, Casemyr NE, Leslie MP, Baumgaertner MR. Implant options for the treatment of intertrochanteric fractures of the hip: rationale, evidence, and recommendations. *Bone Joint J*. (2017) 99-b:128–33. doi: 10.1302/0301-620x.99b1.Bjj-2016-0134.R1

30. Yu X, Wang H, Duan X, Liu M, Xiang Z. Intramedullary versus extramedullary internal fixation for unstable intertrochanteric fracture: a meta-analysis. *Acta Orthop Traumatol Turc*. (2018) 52:299–307. doi: 10.1016/j.aott.2018.02.009

31. Foss NB, Kehlet H. Hidden blood loss after surgery for hip fracture. *J Bone Joint Surg Br*. (2006) 88:1053–9. doi: 10.1302/0301-620x.88b8.17534

32. Jewell DP, Gheduzzi S, Mitchell MS, Miles AW. Locking plates increase the strength of dynamic hip screws. *Injury*. (2008) 39:209–12. doi: 10.1016/j.injury.2007.05.018

33. Medoff RJ, Maes K. A new device for the fixation of unstable pertrochanteric fractures of the hip. *J Bone Joint Surg Am*. (1991) 73:1192–9.

34. Cheng Q, Huang W, Gong X, Wang C, Liang X, Hu N. Minimally invasive percutaneous compression plating versus dynamic hip screw for intertrochanteric fractures: a randomized control trial. *Chin J Traumatol*. (2014) 17:249–55. doi: 10.3760/cma.j.issn.1008-1275.2014.05.001

35. Gotfried Y. Percutaneous compression plating of intertrochanteric hip fractures. *J Orthop Trauma*. (2000) 14:490–5. doi: 10.1097/00005131-200009000-00005

36. Parker MJ, Handoll HH. Gamma and other cephalocondylic intramedullary nails versus extramedullary implants for extracapsular hip fractures in adults. *Cochrane Database Syst Rev*. (2010) 26:Cd000093. doi: 10.1002/14651858.CD000093.pub5

37. Haidukewych GJ. Intertrochanteric fractures: ten tips to improve results. *J Bone Joint Surg Am*. (2009) 91:712–9.

38. Liu Y, Tao R, Liu F, Wang Y, Zhou Z, Cao Y, et al. Mid-term outcomes after intramedullary fixation of peritrochanteric femoral fractures using the new proximal femoral nail antirotation (PFNA). *Injury*. (2010) 41:810–7. doi: 10.1016/j.injury.2010.03.020

39. Horner NS, Samuelsson K, Solyom J, Bjørgul K, Ayeni OR, Östman B. Implant-related complications and mortality after use of short or long gamma nail for intertrochanteric and subtrochanteric fractures: a prospective study with minimum 13-year follow-up. *JB JS Open Access*. (2017) 2:e0026. doi: 10.2106/jbjs.Oa.17.00026

40. Zheng L, Wong DW, Chen X, Chen Y, Li P. Risk of proximal femoral nail antirotation (PFNA) implant failure upon different lateral femoral wall thickness in intertrochanteric fracture: a finite element analysis. *Comput Methods Biomech Biomed Engin*. (2021) 25:1–9. doi: 10.1080/10255842.2021.1964488

41. Chen Y, Wei ZZ, Zhang Kl, Li Z. Biocompatibility comparison between different dynamic hip screws for femoral intertrochanteric fractures. *J Clin Rehabilitative Tissue Eng Res*. (2011) 15:9100–3. doi: 10.3969/j.issn.1673-8225.2011.48.043

42. Rog D, Grigsby P, Hill Z, Pinette W, Inceoglu S, Zuckerman L. A biomechanical comparison of the two- and four-hole side-plate dynamic hip screw in an osteoporotic composite femur model. *J Orthop Surg (Hong Kong)*. (2017) 25:2309499017717199. doi: 10.1177/2309499017717199.

43. Yian EH, Banerji I, Matthews LS. Optimal side plate fixation for unstable intertrochanteric hip fractures. *J Orthop Trauma*. (1997) 11:254–9. doi: 10.1097/00005131-199705000-00003

Publisher's Note: All claims expressed in this article are solely those of the authors and do not necessarily represent those of their affiliated organizations, or those of the publisher, the editors and the reviewers. Any product that may be evaluated in this article, or claim that may be made by its manufacturer, is not guaranteed or endorsed by the publisher.